LITERATURE CITED

Burton, W. K., N. Cabrera, and F. C. Frank, "Growth of Crystals and Equilibrium Structure of Their Surfaces," *Phil. Trans. Roy. Soc. London*, **A 243**, 229 (1951).

Cayey, N. W., and J. Estrin, "Secondary Nucleation in Agitated, Magnesium Sulfate Solutions," *Ind. Eng. Chem. Fundamentals*, **6**, 13 (1967).

Clontz, N. A., and L. W. McCabe, "Contact Nucleation of Magnesium Sulfate Heptahydrate," *Chem. Eng. Progr. Symp. Ser.*, **67**, 6 (1971).

Cooper, T. R., and D. C. Timm, "Crystallization: Kinetics and Design Consideration," *AIChE J.*, **17**, 285 (1971).

Desai, R. M., "The Effect of Crystal Moments on Secondary Nucleation," unpublished M.S. Thesis, Univ. Nebraska-Lincoln (1971).

Hulburt, H. M., and S. Katz, "Continuous Crystallization," *Chem. Eng. Sci.*, **191**, 555 (1964).

Kothari, I. R., "Growth of Single Cells of *Schizosaccharomyces pombe* under Nutrient Limitation," unpublished M. S. Thesis, Univ. Nebraska-Lincoln (1971).

Larson, M. A., D. C. Timm, and P. R. Wolff, "Effect of Suspension Density on Crystal Size Distribution," *AIChE J.*, **14**, 448 (1968).

Powers, H. E. C., "Nucleation and Early Crystal Growth," *Ind. Chem.*, **39**, 351 (1963).

Rachow, J. W., "Steady State Nucleation Kinetics of Aqueous Potasium Dichromate," unpublished M.S. thesis, Univ. Nebraska-Lincoln (1969).

Randolph, A. D., and M. S. Larson, "Transient and Steady State Size Distributions in Continuous Mixed Suspension Crystallizers," *AIChE J.*, **8**, 639 (1962).

Rosen, H. N., and H. M. Hulburt, "Growth Rate of Potassium Sulfate in a Fludized-Bed Crystallizer," *Chem. Eng. Progr. Symp. Ser.*, **67**, 27 (1971).

Shor, S. M., and M. A. Larson, "Effect of Additives of Crystallization Kinetics," *Chem. Eng. Progr. Symp. Ser.*, **67**, 32 (1971).

Strickland-Constable, R. F., *Crystallization*, p. 112, Academic Press, New York (1968).

Ting, H. H., and W. L. McCabe, "Supersaturation and Crystal Formation in Seeded Solution," *Ind. Eng. Chem.*, **26**, 1201 (1934).

Manuscript received May 22, 1973; revision received September 4 and accepted September 5, 1973.

A Theoretical Model for Enzymatic Catalysis Using Asymmetric Hollow Fiber Membranes

The behavior of an immobilized enzyme reactor utilizing asymmetric hollow fibers is simulated using a theoretical model. In this reactor, an enzyme solution contained within the annular open-cell porous support structure of the fiber is separated from a substrate flowing through the fiber lumen by an ultrathin dense membrane impermeable to enzyme but permeable to substrate and product. The coupled set of model equations describing the behavior of this reactor represents an extended Graetz problem in the fiber lumen, with diffusion through the ultrathin fiber skin and reaction in the microporous sponge region. Exact analytic expressions for substrate concentration profiles throughout an idealized fiber which incorporate the membrane and hydrodynamic mass transfer resistances are obtained for a first-order enzyme reaction, and numerical techniques for their evaluation are given. This analysis is extended to yield a numerical finite difference solution for nonlinear Michaelis-Menten reaction kinetics, which is shown to agree with the analytic solution, as K_m/C_0, the ratio of the Michaelis constant to the initial substrate concentration, becomes large (> 100).

LARRY R. WATERLAND
ALAN S. MICHAELS
and
CHANNING R. ROBERTSON

Department of Chemical Engineering
Stanford University
Stanford, California 94305
and the
Alza Research Corporation
Palo Alto, California 94304

SCOPE

In recent years the potential applications of enzymatic catalysis in numerous diverse areas of chemical technology have become apparent. This in turn has brought about a need to develop and characterize new techniques for enzyme immobilization concomitant with the design of efficient immobilized enzyme reactors. Immobilized en-

Correspondence concerning this paper should be addressed to C. R. Robertson.

zymes possess the unique feature of being easily recoverable from a reaction mass, thereby permitting reuse and subsequent economic catalyst utilization. To this end, the use of hollow fiber membranes has received increasing attention. For example, an immobilization technique was recently suggested, and mathematically modeled, by Rony (1971), in which hollow fibers are filled with an enzyme solution and substrate is passed over the fiber exterior; and Horvath et al. (1973) have recently proposed and modeled an open tube heterogeneous enzyme reactor.

In this paper we discuss a new enzyme immobilization technique using asymmetric hollow fiber membranes in which enzyme saturates the microporous sponge section of the fiber wall and substrate is passed through the lumen. With this configuration it is possible to account exactly for the membrane and hydrodynamic diffusional resistances to substrate and product mass transfer. To investigate the manner in which various kinetic and diffusion parameters influence the behavior of a multitube reactor utilizing this type of enzyme placement, a theoretical analysis was developed to simulate the reactor operation under a variety of conditions.

CONCLUSIONS AND SIGNIFICANCE

The performance of a new type of immobilized enzyme reactor using asymmetric hollow fibers has been examined using a theoretical model. Solutions obtained with this model give exact analytic expressions for substrate concentration profiles throughout an idealized fiber for a first-order enzyme reaction. The resulting expressions, however, are not easily evaluated; therefore, a numerical technique for their evaluation has been developed. These analytic and numerical techniques are of general interest for application to problems containing unknown and variable concentrations (temperature) or fluxes at the wall of a cylindrical tube. For generalized Michaelis-Menten enzyme kinetics a numerical finite difference solution is presented.

Model calculations were carried out for parameter values representing a wide range of practical reactor operation. At all levels of substrate conversion, there exist distinct regions of enzyme kinetic control and diffusion control, where, in the latter case, the dimensionless length required to effect a given conversion is essentially independent of enzyme activity. In addition, for typical values of the governing parameters, the ultrathin membrane presents negligible mass transport resistance to reaction. Accordingly, diffusional resistances are confined almost exclusively to the flowing substrate and the excluded enzyme solution. Finite difference calculations for nonlinear kinetics indicate that the transition between conditions of diffusion control and kinetic control occurs over a narrower range of the Thiele modulus as K_m/C_0 decreases. Furthermore, the linear kinetics model accurately describes reactor operation for $K_m/C_0 \geqq 100$.

These theoretical results, which include a complete set of design criteria, strongly suggest that asymmetric hollow fiber reactors provide a potentially attractive means for carrying out chemical conversions requiring enzymes as catalysts.

In recent years numerous techniques have been developed for rendering enzymes insoluble (Goldman et al., 1971; Brown and Hasselberger, 1971; Carbonell and Kostin, 1972; Silman and Katchalski, 1966). The methods most often discussed have focused on binding the protein to an insoluble carrier matrix. These immobilized derivatives, however, invariably suffer decreased enzyme activity due to steric and diffusional limitations. The use of semipermeable microcapsules by Chang et al. (1966), on the other hand, has provided a different approach to enzyme immobilization. Using this procedure, an enzyme solution is trapped within a membrane enclosed capsule having permeability characteristics which retain the protein but permit the passage of small substrate and product components. The primary advantage of this technique is the elimination of steric hindrance and possible deactivation of the enzyme due to binding at or near the active site. However, these advantages are somewhat offset by substantial enzyme denaturation during the interfacial polymerization step essential to microcapsule formation. Also, once the microcapsules have been formed, it is not possible to regenerate or augment the enzyme solution without fabricating additional capsules.

Recently Rony (1971, 1972) proposed an alternate approach to enzyme encapsulation using membrane hollow fibers. Rony suggested that cylindrical microcapsules might be fabricated by filling the lumen of these fibers with an enzyme solution and then sealing the two ends. By forming a bundle of these enzyme-loaded fibers and causing substrate solution to flow over the external fiber surfaces through the inter-fiber passages, substrate conversion into product can be accomplished if the fiber walls are permeable to substrate and product (but not to enzyme). Limitations to this approach, obviously, are (1) the fabrication of hollow fiber membranes with adequately high permeability to substrate and product, and (2) control of fluid flow within the fiber bundle to assure uniform flow distribution and minimize stagnation, and thereby avoid significant diffusional resistance to mass transfer.

These limitations can in large measure be circumvented by reversing Rony's proposed configuration (that is, flowing substrate solution through the fiber-lumen, with enzyme confined externally to the lumen) and utilizing recently-developed noncellulosic asymmetric microporous hollow fibers designed for use in ultrafiltration/dialysis processes. Typical dimensions of these fibers are 350 μm O.D. and 200 μm I.D.; as shown schematically in Figure 1, they are comprised of an approximately 0.5-μm thick semipermeable skin (whose pore size can be controlled in the range of 10-200Å) sheathed by a 75 μm thick, annular open-celled sponge of mean pore size of 5 to 10 μm. This sponge-layer is 80 to 90% void, has very high hydraulic permeability, and serves primarily as a mechanical support for the ultrathin membrane skin lining the fiber lumen. So long as the pores in the skin are too small to pass enzyme molecules but adequately large to freely

pass substrate and product, enzyme confined in the annular space external to the skin layer can act upon substrate molecules delivered by diffusion from solution flowing in the lumen without migration and loss of enzyme. Furthermore, since the resistance to transport of substrate and product offered by the ultrathin skin is exceedingly small compared with their resistance to diffusion in solution, the rate-limiting steps in the conversion process will be either simple diffusion or the kinetics of the enzymatic reaction.

PROPOSED ENCAPSULATION PROCEDURE

Rather than placing the enzyme solution within the fiber lumen, we propose a new configuration in which the enzyme solution saturates the porous sponge section of the fiber wall and substrate is passed through the fiber lumen. Under these conditions, as shown in Figure 2, the enzyme is indeed immobilized or sequestered since, owing to its size, it cannot pass through the matrix of the ultrathin skin. On the other hand, it is prevented from leaving the sponge matrix due to the sponge-gas interface at the shell-side fiber boundary. This configuration serves to minimize mass transfer diffusional resistances, thereby making it a very attractive method for enzyme immobilization since, in particular, the substrate and enzyme solutions are physically separated by only 0.5 μm.

Another very important practical advantage of this type of immobilized enzymatic reactor configuration is the fact that the enzyme is, in reality, only immobilized with respect to the solution flowing in the fiber lumen. By the simple expedient of flushing solution through the annular sponge, it is possible to remove and replace the enzyme (or introduce another enzyme) as desired without dismantling or otherwise disturbing the system. Moreover, this configuration is well suited for the conduct of multienzyme conversions and to the use of highly labile enzymes which cannot tolerate chemical immobilization procedures.

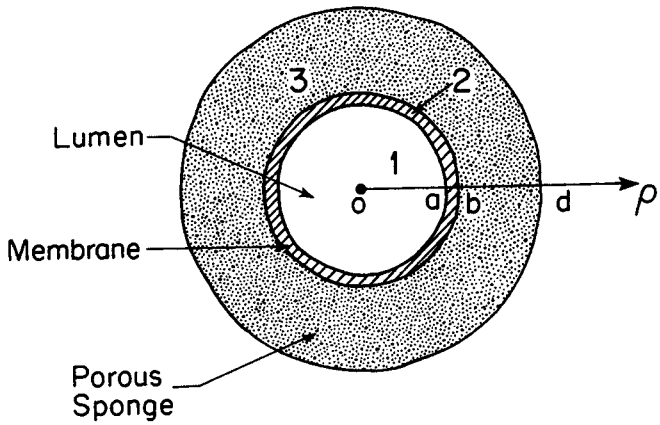

Fig. 1. Asymmetric hollow fiber schematic—radial cross section.

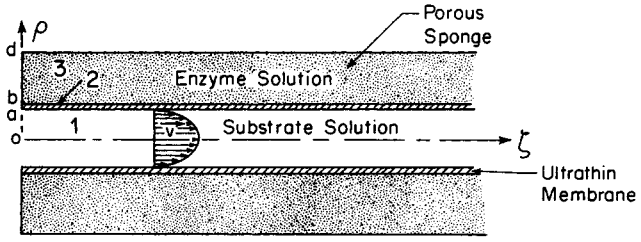

Fig. 2. Asymmetric hollow fiber schematic—axial cross section.

The extrapolation of this approach to a multifiber reactor is obvious. Hollow fiber tube modules containing 1000 to 10,000 asymmetric fibers mounted in a lucite case are readily available (Cross, 1972), and large-scale systems embodying multiple module assemblies are now under development. By saturating the sponge matrix of each fiber with enzyme solution and flowing substrate through each fiber lumen, a compact enzyme reactor results. To examine the behavior of this type of reactor, a mathematical model was developed to complement a parallel experimental program. The paper is concerned only with the model; experimental results will appear in a subsequent publication.

MATHEMATICAL DEVELOPMENT

The idealized asymmetric hollow fiber under consideration is shown in Figure 1. It consists of a cylindrical tube divided into three regions: region 3 is the porous sponge section of the fiber wall, region 2 is the dense ultrathin membrane, and region 1 is the tube lumen. Laminar flow of substrate (and product) is assumed in region 1 with substrate (and product) diffusing throughout each of the three regions. Chemical reaction is confined to region 3 which contains the enzyme solution. This development further assumes steady state conditions and constant fluid properties. Axial diffusion is neglected in all regions, and region 3 is assumed to contain stagnant fluid.

A mathematical model for a reactor of this general configuration was considered recently by Horvath et al. (1973). Horvath's open tube heterogeneous enzyme reactor (OTHER) consists of a tube with an enzyme-matrix coated wall, and the model used to describe its behavior follows from an analysis of a catalytic wall with the wall possessing a finite thickness. In particular, Horvath et al. assumed that the catalytic annulus was sufficiently thin that Cartesian coordinates could be used in the equation describing mass transport in the wall. In contrast, the reactor described herein contains an inert "membrane" region of finite thickness separating the cylindrical core and the catalytic annulus. But of greater importance, the model presented in this report does not neglect curvature effects in the transport equation in the annular catalytic region since the dimensions of a typical asymmetric hollow fiber necessitate the use of cylindrical coordinates. In addition, Horvath et al. uncoupled the governing differential equations by defining an effectiveness factor and solved the resulting nonlinear equations numerically. Here, the coupled equations are solved directly, and for a first-order enzyme reaction, analytic solutions are given.

Utilizing the above assumptions, the governing differential equations for the substrate concentration in each region are

$$\mathcal{D}_3 \frac{1}{\rho}\frac{\partial}{\partial \rho}\left(\rho \frac{\partial C_3^*}{\partial \rho}\right) = R \qquad (1)$$

$$\mathcal{D}_2 \frac{1}{\rho}\frac{\partial}{\partial \rho}\left(\rho \frac{\partial C_2^*}{\partial \rho}\right) = 0 \qquad (2)$$

$$\mathcal{D}_1 \frac{1}{\rho}\frac{\partial}{\partial \rho}\left(\rho \frac{\partial C_1^*}{\partial \rho}\right) = v_z \frac{\partial C_1^*}{\partial \zeta} \qquad (3)$$

where $v_z(\rho)$ is the velocity profile in region 1, which, for laminar flow, is

$$v_z = v_0\left(1 - \frac{\rho^2}{a^2}\right) \qquad (4)$$

The rate of the enzyme reaction in region 3 is usually described by the Michaelis-Menten expression:

$$R = \frac{V_{max} C_3^*}{K_m + C_3^*} \tag{5}$$

Use of this relation, however, precludes a simple solution to (1). There are, however, two limiting forms to (5) which offer significant simplification: a zero-order reaction for $C_3^* >> K_m$ and a first-order reaction for $C_3^* << K_m$. The problem is initially solved for a first-order reaction in region 3. This condition may be attained in any experimental situation provided that C_3^* is sufficiently small. Subsequently a numerical solution is presented for the nonlinear reaction case with Michaelis-Menten kinetics in region 3.

Using the dimensionless coordinates $r = \rho/a$ and $z = \zeta/a\alpha$, where

$$\alpha = \frac{v_0 a}{\mathcal{D}_1} \tag{15}$$

is the Péclet number, with concentrations $C_i = C_i^*/C_0$ $(i = 1, 2, 3)$, and $f = C_w^*/C_0$, and a Thiele modulus

$$\lambda^2 = \frac{V_{max} a^2}{K_m \mathcal{D}_3} \tag{16}$$

the solutions to (2) and (6) satisfying boundary conditions (7) to (10) are found to be

$$C_3(r,z) = \frac{\gamma \mathcal{D}_2 a}{\gamma \mathcal{D}_2 a \left[K_0\left(\frac{\lambda b}{a}\right) I_1\left(\frac{\lambda d}{a}\right) + K_1\left(\frac{\lambda d}{a}\right) I_0\left(\frac{\lambda b}{a}\right) \right] + \mathcal{D}_3 b\lambda \ln \frac{b}{a} \left[K_1\left(\frac{\lambda b}{a}\right) I_1\left(\frac{\lambda d}{a}\right) - K_1\left(\frac{\lambda d}{a}\right) I_1\left(\frac{\lambda b}{a}\right) \right]}$$
$$\left\{ I_1\left(\frac{\lambda d}{a}\right) K_0(\lambda r) + K_1\left(\frac{\lambda d}{a}\right) I_0(\lambda r) \right\} \cdot f(z) \tag{17}$$

$$C_2(r,z) = \left\{ 1 - \frac{\mathcal{D}_3 \lambda b \left[K_1\left(\frac{\lambda b}{a}\right) I_1\left(\frac{\lambda d}{a}\right) - K_1\left(\frac{\lambda d}{a}\right) I_1\left(\frac{\lambda b}{a}\right) \right] \ln r}{\gamma \mathcal{D}_2 a \left[K_0\left(\frac{\lambda b}{a}\right) I_1\left(\frac{\lambda d}{a}\right) + K_1\left(\frac{\lambda d}{a}\right) I_0\left(\frac{\lambda b}{a}\right) \right] + \mathcal{D}_3 b\lambda \ln \frac{b}{a} \left[K_1\left(\frac{\lambda b}{a}\right) I_1\left(\frac{\lambda d}{a}\right) - K_1\left(\frac{\lambda d}{a}\right) I_1\left(\frac{\lambda b}{a}\right) \right]} \right\}$$
$$\cdot \gamma f(z) \tag{18}$$

First-Order Kinetics

For a first-order enzyme reaction, (1) becomes

$$\mathcal{D}_3 \frac{1}{\rho} \frac{\partial}{\partial \rho} \left(\rho \frac{\partial C_3^*}{\partial \rho} \right) = \frac{V_{max}}{K_m} C_3^* \tag{6}$$

The appropriate boundary conditions for (2), (3), and (6) are

$$\left. \frac{\partial C_3^*}{\partial \rho} \right|_{\rho=d} = 0 \tag{7}$$

$$\gamma C_3^*(b, \zeta) = C_2^*(b, \zeta) \tag{8}$$

$$\mathcal{D}_3 \left. \frac{\partial C_3^*}{\partial \rho} \right|_{\rho=b} = \mathcal{D}_2 \left. \frac{\partial C_2^*}{\partial \rho} \right|_{\rho=b} \tag{9}$$

$$C_2^*(a, \zeta) = \gamma C_w^*(\zeta) \tag{10}$$

$$\mathcal{D}_2 \left. \frac{\partial C_2^*}{\partial \rho} \right|_{\rho=a} = \mathcal{D}_1 \left. \frac{\partial C_1^*}{\partial \rho} \right|_{\rho=a} \tag{11}$$

$$C_1(a, \zeta) = C_w^*(\zeta) \quad \zeta > 0 \tag{12}$$

$$C_1^*(\rho, \zeta) = C_0 \quad \zeta < 0 \tag{13}$$

$$\left. \frac{\partial C_1^*}{\partial \rho} \right|_{\rho=0} = 0 \tag{14}$$

Equation (7) requires that substrate does not leave the outer boundary of the fiber sponge. This assumption is clearly valid for a single, isolated fiber with enzyme solution localized in the porous sponge region; however, it should also apply to a fiber bundle, assuming the fibers are in a somewhat cylindrically close-packed array. Equations (8), (10), and (12) relate concentrations across region boundaries through the membrane partition coefficient γ. The wall concentration $C_w^*(\zeta)$ is assumed to be an arbitrary, well-behaved, but known function of ζ, its purpose being to simplify the solution of (3). It will be determined as part of the overall solution to the problem. Equations (9) and (11) relate mass fluxes across region boundaries, (13) is an initial condition at the reactor inlet, and (14) provides for axial symmetry.

In dimensionless form, (3) and boundary conditions (12) to (14) become

$$\frac{\partial^2 C_1}{\partial r^2} + \frac{1}{r} \frac{\partial C_1}{\partial r} - (1 - r^2) \frac{\partial C_1}{\partial z} = 0 \tag{19}$$

$$C_1(1, z) = f(z) \quad z > 0 \tag{20}$$

$$C_1(r, z) = 1 \quad z < 0 \tag{21}$$

$$\left. \frac{\partial C_1}{\partial r} \right|_{r=0} = 0 \tag{22}$$

Equation (19) with boundary conditions (20) to (22) does not yield an immediate analytic solution. Therefore, consider first the analogous Graetz problem which results when (20) is replaced by the homogeneous form:

$$C_1(1, z) = 0 \quad z > 0 \tag{20a}$$

This problem, (19), (20a), (21), and (22), is now in Sturm-Liouville form. The solution $C_h(r, z)$ will be called the homogeneous solution:

$$C_h(r, z) = \sum_{n=0}^{\infty} A_n R_n(r) \exp(-\beta_n^2 z) \tag{23}$$

where β_n and R_n are the eigenvalues and eigenfunctions, respectively, of the equation

$$r \frac{d^2R}{dr^2} + \frac{dR}{dr} + \beta^2 r(1 - r^2) R = 0$$
$$R(1) = 0 \tag{24}$$
$$R'(0) = 0$$

with the coefficients given by

$$A_n = \frac{\int_0^1 r(1 - r^2) R_n(r)\, dr}{\int_0^1 r(1 - r^2) R_n^2(r)\, dr} \tag{25}$$

An asymptotic solution to the Graetz problem for large β_n providing accurate values of the eigenfunctions $R_n(r)$ has been obtained by Sellars et al. (1956); and Brown (1960) has tabulated the first six eigenfunctions. These two solutions can be shown to match at $n = 6$; hence expressions are readily available for A_n and $R_n(r)$. The most accurate evaluation of the eigenvalues is provided by Brown (1960) for $n < 12$ and by Lauwerier (1951) for $n \geq 12$.

The solution to (19) to (22) can now be obtained simply by superposing the Graetz solutions (23), resulting in a Stieltjes integral formulation:

$$C_1(r, z) = 1 + \int_0^z \frac{df(\xi)}{d\xi} \left\{ 1 - \sum_{n=0}^{\infty} A_n R_n(r) \exp\left[-\beta_n^2(z - \xi)\right] \right\} d\xi \quad (26)$$

The wall concentration $f(z)$ is found from (11) to be

$$f(z) = \sigma \int_0^z \frac{df(\xi)}{d\xi} \left\{ \sum_{n=0}^{\infty} A_n \left.\frac{dR_n(r)}{dr}\right|_{r=1} \exp\left[-\beta_n^2(z - \xi)\right] \right\} d\xi \quad (27)$$

for $z > 0$, with $f(0) = 1$, and

$$\sigma = \frac{\gamma \mathcal{D}_2 \mathcal{D}_1 a \left[K_0\left(\frac{\lambda b}{a}\right) I_1\left(\frac{\lambda d}{a}\right) + K_1\left(\frac{\lambda d}{a}\right) I_0\left(\frac{\lambda b}{a}\right) \right] + \mathcal{D}_3 \mathcal{D}_1 b \lambda \ln\frac{b}{a} \left[K_1\left(\frac{\lambda b}{a}\right) I_1\left(\frac{\lambda d}{a}\right) - K_1\left(\frac{\lambda d}{a}\right) I_1\left(\frac{\lambda b}{a}\right) \right]}{\gamma \mathcal{D}_3 \mathcal{D}_2 b \lambda \left[K_1\left(\frac{\lambda b}{a}\right) I_1\left(\frac{\lambda d}{a}\right) - K_1\left(\frac{\lambda d}{a}\right) I_1\left(\frac{\lambda b}{a}\right) \right]} \quad (28)$$

Since it is not possible to explicitly obtain $f(z)$ from (27), a numerical technique must be employed. Wissler and Schechter (1962) proposed a numerical scheme for Volterra integral equations of this type; however, we have presented an alternate technique in Appendix A* which was found to be computationally more efficient for this problem.

Nonlinear Kinetics

Since the assumption of first-order enzyme kinetics, in general, greatly limits the range of inlet substrate concentrations ($C^* << K_m$), it is of interest to solve the governing equations with the full Michaelis-Menten rate expression. Substituting (5) into (1) and defining

$$\theta = \frac{K_m}{C_0} \quad (29)$$

$$\varphi = \lambda^2 \theta \quad (30)$$

the diffusion equation for region 3 becomes

$$\frac{\partial^2 C_3}{\partial r^2} + \frac{1}{r}\frac{\partial C_3}{\partial r} = \frac{\varphi C_3}{\theta + C_3} \quad (31)$$

Equations (2) and (3) for regions 2 and 1, and boundary conditions (7) to (14) remain.

Equation (31) is nonlinear, however, and possesses no analytic solution; therefore, an iterative numerical solution to (2), (3), (7) to (14), and (31) was developed.

The solution to (2) using (10) and (11) is

$$C_2(r, z) = \frac{\mathcal{D}_1}{\mathcal{D}_2} Q_1(z) \ln r + \gamma f(z) \quad (32)$$

where

$$Q_1(z) = \left.\frac{\partial C_1}{\partial r}\right|_{r=1} \quad (33)$$

Using (8) gives the relation

$$C_3\left(\frac{b}{a}, z\right) = \frac{\mathcal{D}_1}{\gamma \mathcal{D}_2} Q_1(z) \ln\frac{b}{a} + f(z) \quad (34)$$

and (9) yields

$$Q_1(z) = \frac{\mathcal{D}_3}{\mathcal{D}_1}\frac{b}{a} Q_3(z) \quad (35)$$

where

$$Q_3(z) = \left.\frac{\partial C_3}{\partial r}\right|_{r=\frac{b}{a}} \quad (36)$$

hence

$$f(z) = C_3\left(\frac{b}{a}, z\right) - \frac{\mathcal{D}_3}{\gamma \mathcal{D}_2}\frac{b}{a} Q_3(z) \ln\frac{b}{a} \quad (37)$$

To solve the complete nonlinear, coupled problem an implicit finite difference scheme is utilized for (19) with (20) through (22), where, at each z_i the following iterative procedure is used:

1. Guess $f(z_i) = f(z_{i-1})$
2. Solve for $C_1(r, z_i)$ numerically
3. Calculate $Q_1(z_i)$
4. Use (34) to calculate $C_3\left(\frac{b}{a}, z_i\right)$
5. Solve (31) using an iterative scheme for nonlinear ordinary differential equations to obtain $C_3(r, z_i)$
6. Calculate $Q_3(z_i)$
7. Refine the guess for $f(z_i)$ from (37).

RESULTS

First-Order Kinetics

Using the first-order reaction model, the tube substrate concentration profile $C_1(r, z)$ may be calculated as a function of six dimensionless parameters: λ^2, z, b/a, d/a, $\mathcal{D}_1/\mathcal{D}_3$, and $\mathcal{D}_1/\gamma\mathcal{D}_2$. Due to the large pore size and high void volume of the fiber sponge, the difference between $\mathcal{D}_1$ and $\mathcal{D}_3$ will be insignificant. However, even this assumption leaves $C_1(r, z)$ a function of five parameters. Therefore, to illustrate the essential predictions of the first-order model, $C_1(r, z)$ was studied only as a function of λ^2 and z. The geometric parameters were set according to the dimensions of a typical asymmetric hollow fiber, the membrane partition coefficient was assumed to be unity, and $\mathcal{D}_2$ was assumed to be an order of magnitude lower than the solution diffusivity, $\mathcal{D}_1$. For all calculations presented herein

$$a = 100\ \mu\text{m}$$

$$b = 100.5\ \mu\text{m}$$

$$d = 175\ \mu\text{m}$$

Appendix A has been deposited as Document No. 02293 with the National Auxiliary Publications Service (NAPS), c/o Microfiche Publications, 305 E. 46 St., N. Y., N. Y. 10017 and may be obtained for $1.50 for microfiche or $5.00 for photocopies.

$$\frac{\mathcal{D}_1}{\mathcal{D}_3} = 1.0$$

$$\frac{\mathcal{D}_1}{\gamma\mathcal{D}_2} = 10$$

The last assumption was found to be easily relaxed. With all other parameters at their set values, varying $\mathcal{D}_1/\gamma\mathcal{D}_2$ from 5 to 20 produced negligible differences in predicted concentration profiles over the range of kinetic and flow parameters investigated. This strongly suggests that the 0.5-μm thick dense membrane region presents negligible diffusional resistance to reactor operation.

With the Thiele modulus and the Péclet number remaining as adjustable parameters, it was found convenient to express predicted results in terms of the bulk concentration C_B as a function of the Thiele modulus λ^2 and the dimensionless reactor length z where

$$C_B(z) = \frac{\int_0^1 2\pi r v_z C_1(r,z)\,dr}{\int_0^1 2\pi r v_z\,dr} = 4\int_0^1 r(1-r^2)C_1(r,z)\,dr \quad (38)$$

In Figure 3 C_B is plotted as a function of log (λ^2) with z as a parameter. The ranges of λ^2 and dimensionless length illustrated encompass essentially the entire range of practical reactor operating conditions. Of particular interest are the two limiting cases for reactor operations: (a) diffusion control and (b) enzyme kinetic control. Figure 3 shows the diffusion controlled asymptotic bulk concentration C_B that is attained for a given dimensionless reactor length as λ^2 becomes large. The kinetically controlled asymptote as λ^2 approaches zero, is $C_B \equiv 1$ for all values of the dimensionless length.

Figure 4, however, is more illustrative. This plot shows the dimensionless length required to effect a given conversion $X = 1 - C_B$ as a function of λ^2. For a large Thiele modulus, a diffusion controlled limit is reached where the required dimensionless length becomes essentially independent of λ^2. Under these conditions, increasing the activity or amount of the catalyst has little effect on the dimensionless length required to obtain a given conversion. Equivalently, given a reactor of fixed dimensionless length, reactor conversion does not significantly increase with increasing catalyst activity or concentration. This point is particularly applicable to enzyme catalysis since the activity of an enzyme invariably decays with time. Accordingly, if initial reactor operation is in a diffusion controlled regime, enzyme activity can decrease to 10%, or even 1%, of initial activity with but a small effect on reactor conversion. This simple notion quite clearly indicates that reactor operation in a partially or totally diffusion controlled regime might lead to an incorrect determination of enzyme stability; that is, a significant decline in V_{max} for for the enzyme would either go undetected or appear to be less than is actually the case under conditions where diffusional processes are to some degree controlling the reactor operation. It is, therefore, imperative to be assured that the overall reaction rate is not limited by diffusion when attempting to assess enzyme stability.

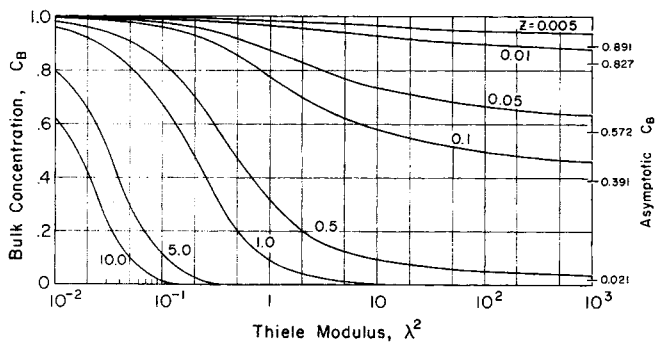

Fig. 3. Predicted bulk substrate concentrations as a function of Thiele modulus at different reactor dimensionless lengths for first-order enzyme kinetics.

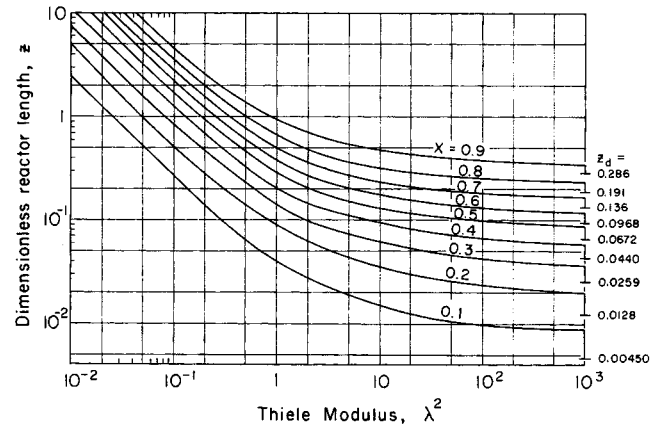

Fig. 4. Relationship between dimensionless reactor length and Thiele modulus as a function of conversion for first-order enzyme kinetics.

At the other extreme, for small λ^2 the kinetically controlled limit obtains as the curves approach straight line asymptotes of log z versus log (λ^2). These results agree qualitatively quite well with those obtained by Horvath et al. (1973) using the OTHER model. This is to be expected due to the similarity of reactor configurations, however, it should again be stressed that there are significant differences between the hollow fiber enzyme reactor proposed herein and Horvath's OTHER, both in the physical configuration and the methods used to analyze the reactor performance. As a consequence, quantitative agreement between the predictions presented herein and those of Horvath et al. for the first-order kinetics limit ($\theta > 100$) are not realized except in the diffusion controlled limit as λ^2 approaches infinity. In particular, the OTHER model predicts substantially different conversions at the same operating parameters than the model presented here. This is due to the fact that, for the hollow fiber geometry, curvature effects cannot be neglected in the catalytic sponge region.

Figure 4 also illustrates the point that in applications where the product is easily separated from the reactor effluent stream, operation at small dimensionless lengths, at the sacrifice of lowered conversion, is desirable. For example, if the dimensional reactor length is held fixed and λ^2 is chosen to be unity, an order of magnitude increase in flow rate would decrease the dimensionless length z by a similar amount thereby reducing reactor conversion by a factor of 4.5. In spite of this reduced conversion, product mass flow rate is increased approximately twofold.

Denoting, for a given conversion, the length at which diffusion control is reached as z_d, the degree of diffusion control η may be defined as

$$\eta = \frac{z_d}{z} \quad (39)$$

which is directly analogous to Horvath's transport effectiveness factor. In agreement with Horvath's findings, Figure 4 shows that for $\eta \leq 0.1$ the reactor is essentially kinetically controlled; therefore, η is indeed a good index for assessing the degree of diffusion control under a given set of operating conditions. It should be noted that η is particularly easy to compute without any prior knowledge of the enzyme kinetics since z_d is readily estimated from the Graetz solution $C_h(r, z)$. For illustration, the z_d at each conversion is shown in Figure 4, and indeed for $z > 10\ z_d$, kinetic control is approached. Furthermore, it should be noted, in contrast to the findings of Horvath et al., that full diffusion control does not obtain even at $\lambda^2 = 1000$. The equivalent diffusion limited bulk concentrations for several dimensionless lengths are shown in Figure 3.

It is also of interest to examine the radial concentration profiles predicted by this model for each limiting case.

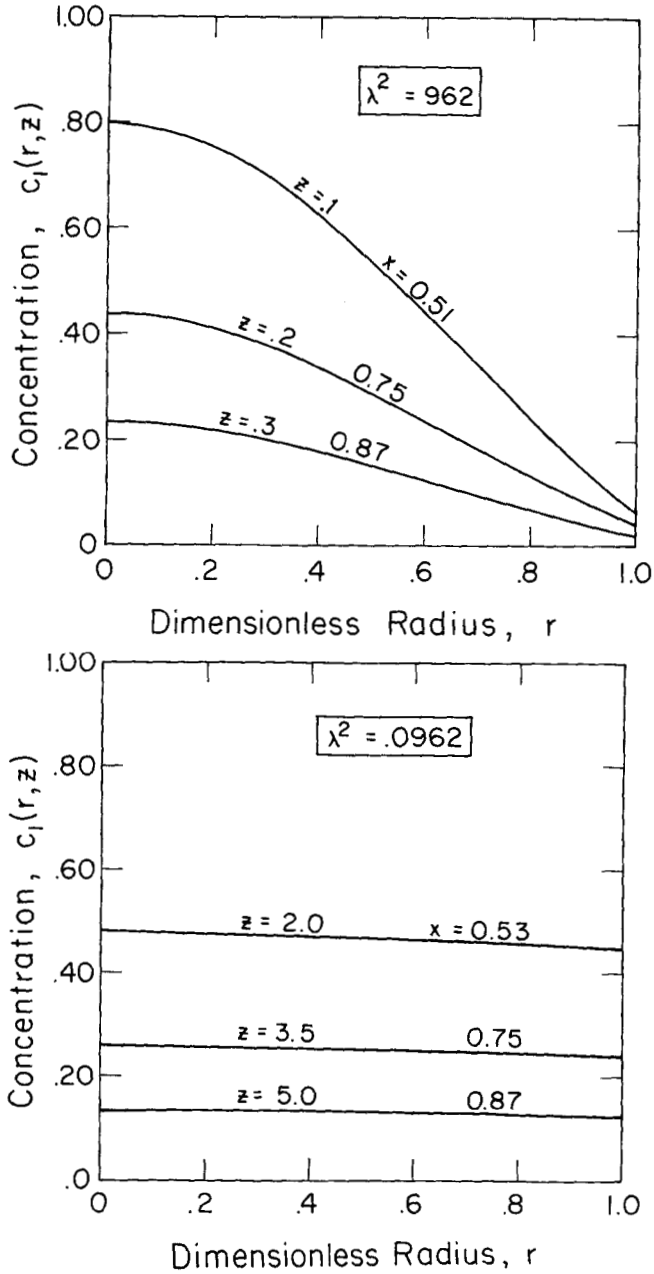

Fig. 5. Radial concentration profiles for several conversions under conditions of (a) diffusion control and (b) kinetic control for first order enzyme kinetics.

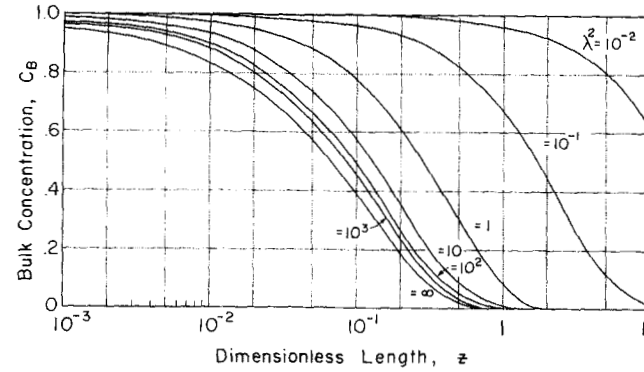

Fig. 6. Axial bulk concentration profiles at varying Thiele modulus for first-order enzyme kinetics.

Figure 5a shows radial concentration profiles under conditions of diffusion control, and Figure 5b shows radial profiles, at essentially the same conversions, under conditions of kinetic control. As would be expected under diffusion control, the concentrations fall sharply with radius, approaching zero at the tube wall, whereas the radial profiles are essentially flat with kinetic control.

Shown in Figure 6 is the relationship between C_B and dimensionless length with λ^2 as a parameter, the curves representing axial bulk concentration profiles as a function of the Thiele modulus. Again the diffusion control limit is observed where the profiles collapse together at large λ^2. As can be seen, the most rapid conversion of substrate occurs as conditions of diffusion control are approached, hence reactor operation in this regime, if feasible, is desirable.

Nonlinear Kinetics

In addition to the six parameters required to describe reactor behavior for first-order kinetics, the substrate concentration profiles for nonlinear Michaelis-Menten kinetics in region 3 also depend on the dimensionless parameter θ. To illustrate the essential predictions of the model, $C_1(r, z)$ was computed only as a function of λ^2, z, and θ, the remaining parameters being held at the values used for the linear kinetics results.

The predicted profiles for the nonlinear case qualitatively resemble those obtained with the first-order model. The same regions of diffusion and kinetic control are seen in Figure 7 for θ varying from 10^{-2} to 10^2 where, in the latter case, operation is essentially described by the linear model. Again qualitative agreement with the OTHER model is observed. In particular, as θ decreases, the transition region between conditions of diffusion control and kinetic control occurs over a narrower range of the Thiele modulus, the region of kinetic control extends to a larger Thiele modulus, and the limiting log z versus log (λ^2) slope for kinetic control increases. These last two observations indicate that an increase in feed concentration may shift reactor operation from a largely diffusion controlled regime to one which is kinetically controlled, with a concomitant decrease in reactor conversion. Equivalently, an increase in feed concentration would require a disproportionate increase in reactor dimensionless length to achieve the same conversion.

CONCLUDING REMARKS

It seems appropriate to compare the reactor configuration proposed herein (enzyme-shell) with its inverse (enzyme-tube) where, in the latter case, the lumen of each

hollow fiber is filled with enzyme solution and substrate is passed through the shell as suggested by Rony (1971, 1972). Unfortunately, the model proposed by Rony is not uniformly applicable for comparison with the work described herein owing to the use of a fictitious film layer to account for the hydrodynamic resistance to mass transfer in the region exterior to the film. To correctly account for this resistance, it is necessary to specify the geometry of the fiber assemblage. Accordingly, an idealized geometrical configuration was selected in which the fibers comprising the bundle are assumed to be arranged in an equilateral triangular array such that each fiber is equidistant from six adjacent fibers. Fluid in laminar flow occupies the interfiber spaces and stagnant enzyme solution fills each fiber lumen.

The appropriate mass transport equations for this enzyme-tube case are developed in Appendix B. For illustration, Figure 8 shows the results obtained with $\theta = 1.0$. The scales for the ordinate and abscissa in this figure were chosen to facilitate direct comparison with Figure 7b based on an equivalent weight of enzyme per fiber with each reactor at the same feed flow rate. Accordingly, the ordinate of Figure 8 is

$$z = z_t \frac{\alpha_t}{\alpha} \tag{40}$$

to account for the fact that $\alpha_t < \alpha$ due to the increased cross-sectional area for flow in the enzyme-tube configuration. Similarly, since the comparison is being made based on an equivalent weight of enzyme per fiber, the abscissa in Figure 8 becomes

$$\lambda^2 = \lambda_t^2 \frac{\text{tube volume}}{\text{shell volume}} \tag{41}$$

Using these two coordinate scalings, enzyme-tube predictions are plotted in enzyme-shell coordinates, thereby allowing direct comparison between the tube and shell configurations.

Examination of Figures 7b and 8 indicate, as expected, that the two configurations respond similarly under conditions of kinetic control. However, under conditions of partial or total diffusion control the enzyme-shell configuration appears to be superior. As the Thiele modulus increases, the dimensionless reactor length required to effect a given conversion for the enzyme-shell configuration decreases relative to that required for the enzyme-tube configuration. A corollary to this is that total diffusion control ($\eta = 1$) is reached at a lower value of λ^2 with the tube configuration as compared to the shell configuration.

These theoretical considerations strongly support the notion that asymmetric hollow fibers containing enzymes in their macroporous walls provide a novel reactor arrangement for effectively carrying out a wide variety of chemical conversions. A few of the advantages of this configuration include:

An enormous surface area to reactor volume ratio,

A hydrodynamically free-shear environment for the enzyme system,

Reactant selectivity by using dense membranes having dissimilar permeability or fixed charge characteristics,

Protection of the enzyme from macromolecular contaminants in the feed stream such as proteolytic enzymes,

An in situ separation of product and enzyme,

Immobilization in soluble form for highly labile enzymes, and

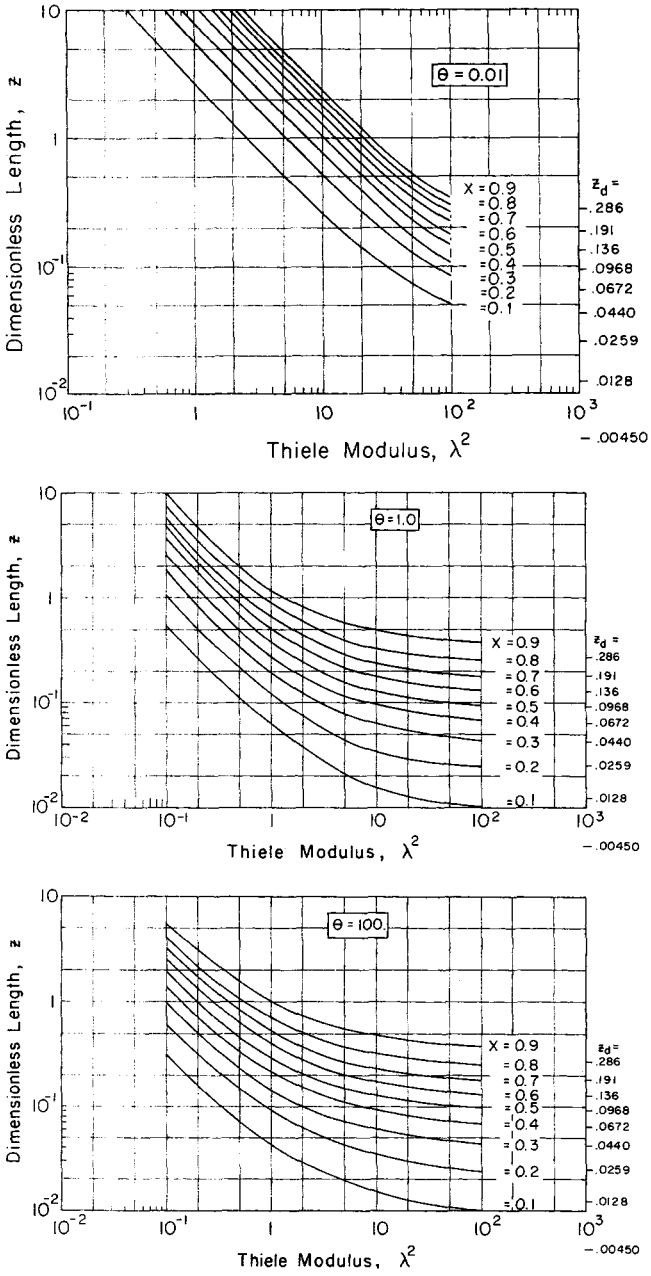

Fig. 7. Relationship between dimensionless reactor length and Thiele modulus as a function of conversion for Michaelis-Menten enzyme kinetics for the enzyme-shell reactor. a) $\theta = 10^{-2}$, b) $\theta = 1.0$, c) $\theta = 10^2$

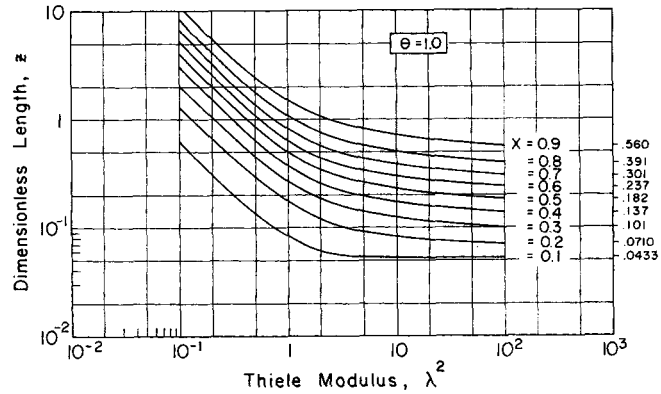

Fig. 8. Relationship between dimensionless reactor length and Thiele modulus as a function of conversion for Michaelis-Menten enzyme kinetics for the enzyme-tube reactor. $\theta = 1.0$

Ease of enzyme regeneration or replacement.

Throughout this report the enzyme has been regarded as a soluble species uniformly distributed and confined within the macroporous open cell region of the asymmetric fiber wall. This, however, does not exclude the possibility of coupling the enzyme to an inert support such as soluble dextran or albumin prior to sequestration within the fiber sponge. As is evidenced by a wide variety of attempts at enzyme immobilization there may be circumstances wherein binding of the enzyme has resulted in greater stability, that is, the time averaged enzyme activity under reaction conditions exceeds that for the soluble and unbound counterpart. Unfortunately, increased stability will not always be observed; hence it is necessary to consider alternative reactor designs whereby soluble immobilized enzymes are utilized. In the case of reactions requiring one or more low molecular weight co-enzymes, however, there appears to be little choice other than to bind the co-enzyme in some manner to an inert support or to the hollow fiber material itself. It should also be noted that even in the hollow fiber reactor considered herein, some degree of denaturation or stabilization could conceivably result by preferential adsorption of the enzyme to the noncellulosic polymer material which forms the fiber sponge. There are still other possibilities such as entrapping the enzyme in a polymer matrix formed within the porous sponge region or utilizing trapped whole cells thereby permitting multienzymic conversions involving several intracellular enzymes. In essence then, this hollow fiber reactor is amenable to all the usual enzyme immobilization techniques and, in fact, provides a common ground of direct comparison among them for any particular enzyme system.

Although the analysis presented in this report deals exclusively with single-enzyme systems and kinetics which are uncomplicated by inhibition considerations, the extension of these ideas to complex multienzyme systems appears to be quite feasible. Another consideration which might bear on this issue is the degree to which substrate and product are convected across the ultrathin skin as a result of ultrafiltration or osmosis. Should either of these mechanisms contribute in a substantial manner to solute and water transport, the analysis described in the previous sections would not be expected to apply unless suitable modifications are introduced. Also, to the extent that enzyme degradation would alter the reactor characteristics, this analysis may be used to qualitatively predict the performance changes to be expected under such conditions. The results presented hopefully provide the requisite basis for further exploration of the hollow fiber geometry to immobilized enzyme technology.

ACKNOWLEDGMENT

The authors wish to acknowledge the Stanford University Research Development Fund for partial support of this research and the National Science Foundation for support in the form of a traineeship held by L. R. Waterland.

NOTATION

a = inner radius of fiber, cm
A_n = constant in the Graetz solution, Equation (25)
b = $(b - a)$ is the thickness of the membrane region of the wall, cm
C = substrate concentration
C_h = solution to Graetz problem
d = $(d - b)$ is the thickness of the sponge region of the fiber wall, cm
$\mathcal{D}$ = substrate diffusivity, cm^2/s
f = C_w^*/C_0, dimensionless substrate wall concentration
F = flow rate, ml/s
I_0 = modified Bessel function of the first kind of order 0
I_1 = modified Bessel function of the first kind of order 1
k = constant, Equation (B5)
K_0 = modified Bessel function of the second kind of order 0
K_1 = modified Bessel function of the second kind of order 1
K_m = Michaelis constant, mole/cm^3
r = ρ/a, dimensionless radial coordinate
r_e = equivalent radius of free shear surface
R = reaction rate, mole/cm^3 · s
R_n = Graetz eigenfunction
v_0 = maximum velocity, cm/s
v_z = velocity, cm/s
V_{max} = maximum enzyme reaction rate, mole/cm^3 · s
X = reactor conversion
z = $\zeta/a\alpha$, dimensionless axial coordinate
z_d = dimensionless length for diffusion controlled reactor

Greek Letters

α = $v_0 a/\mathcal{D}_1$, Péclet number, Equation (15)
α_t = $kFa^3/\pi(r_e^2 - a^2)\mathcal{D}_4$, Péclet number, Equation (B-20)
β_n = Graetz eigenvalue
γ = membrane partition coefficient
ζ = axial coordinate, cm
η = z_d/z, degree of diffusion control
θ = K_m/C_0
λ^2 = $V_{max}a^2/K_m\mathcal{D}_3$, Thiele modulus
ξ = dummy variable of integration
ρ = radial coordinate, cm
σ = constant, Equation (28)
φ = $\lambda^2\theta$

Superscripts

$'$ = differentiation
$*$ = dimensional quantity

Subscripts

0 = inlet
1, 2, 3, 4 = region
B = bulk
t = parameter for the "enzyme-tube" configuration
w = wall

LITERATURE CITED

Brown, G. M., "Heat or Mass Transfer in a Fluid in Laminar Flow in a Circular or Flat Conduit," *AIChE J.*, **6**, 179 (1960).

Brown, H. D., and F. X. Hasselberger, "Matrix-Supported Enzymes," in *Chemistry of the Cell Interface*, Part B, H. D. Brown (ed.), p. 185, Academic Press, N. Y. (1971).

Carbonell, R. G., and M. D. Kostin, "Enzyme Kinetics and Engineering," *AIChE J.*, **18**, 1 (1972).

Chang, T. M. S., F. C. McIntosh, and S. G. Mason, "Semipermeable Aqueous Microcapsules," *Can. J. Physiol. Pharm.*, 44, 115 (1966).

Cross, R. A., "Asymmetric Hollow Fibers for Ultrafiltration and Dialysis," *AIChE Symp. Ser. No. 120*, **68**, 15 (1972).

Goldman, R., L. Goldstein, and E. Katchalski, "Water-Insoluble Enzyme Derivatives and Artificial Enzyme Membranes," in *Biomedical Aspects of Reactions at Solid Surfaces*, p. 1, G. R. Stark (ed.), Academic Press, N. Y. (1971).

Horvath, C., L. H. Shendalman, and R. T. Light, "Open Tubular Heterogeneous Enzyme Reactors: Analysis of a Theoretical Model," *Chem. Eng. Sci.*, **28**, 375 (1973).
Lauwerier, H. A., "The Use of Confluent Hypergeometric Functions in Mathematical Physics and the Solution of an Eigenvalue Problem," *Appl. Sci. Res.*, **A2**, 184 (1951).
Rony, P. R., "Multiphase Catalysis II. Hollow Fiber Catalysts," *Biotech. Bioeng.*, **13**, 431 (1971).
———., "Hollow Fiber Enzyme Reactors," *J. Am. Chem. Soc.*, **94**, 8247 (1972).
Sellars, J. R., M. Tribus, and J. S. Klein, "Heat Transfer to Laminar Flow in a Round Tube or Flat Conduit—The Graetz Problem Extended," *Trans. ASME*, **78**, 441 (1956).
Silman, I. H., and E. Katchalski, "Water-Insoluble Derivatives of Enzymes, Antigens, and Antibodies," *Ann. Rev. Biochem.*, **35**, 873 (1966).
Wissler, E. H., and R. S. Schecter, "Turbulent Flow of Gas Through a Circular Tube with Chemical Reaction at the Wall," *Chem. Eng. Sci.*, **17**, 937 (1962).

APPENDIX B

To model the enzyme-tube configuration proposed by Rony so as to afford comparison with the enzyme-shell configuration, a number of assumptions concerning the geometry of a hollow fiber module are required. The fibers comprising the module are assumed to be arranged in an equilateral triangular array so that each fiber is equidistant from six other fibers as shown in Figure B1. Thus, for axial laminar flow of fluid through the interfiber region in the absence of ultrafiltration a hexagonal free shear surface would ideally be expected to surround each fiber. For further simplification this hexagonal cell is approximated by a cylinder of equivalent radius r_e, this being the radius of a circle whose area is equivalent to that of the hexagon. The equations of motion for the reactant fluid in region 4 then become analogous to those of a falling film.

$$\frac{1}{r}\frac{d}{dr}\left(r\frac{dv_z}{dr}\right) = 4k \tag{B1}$$

$$v_z\Big|_{r=\frac{d}{a}} = 0 \tag{B2}$$

$$\frac{dv_z}{dr}\Big|_{r=\frac{r_e}{a}} = 0 \tag{B3}$$

where the constant k is proportional to the Reynolds number and to the axial pressure drop. Equation (B2) specifies the no slip condition at the fiber boundary and Equation (B3) denotes the free shear surface. The solution to Equations (B1) to (B3) is

$$v_z = k\left(r^2 - \frac{d^2}{a^2} - 2\frac{r_e^2}{a^2}\ln\frac{ra}{d}\right) \tag{B4}$$

where k is given by

$$k = \left\{\frac{3r_e^2 + d^2}{2a^2} - \frac{2r_e^4}{r_e^2 - r_o^2}\ln\frac{r_e}{r_o}\right\}^{-1} \tag{B5}$$

The mass transport equations for each fiber are directly analogous to those used to describe the enzyme-shell configuration.

$$\frac{1}{r}\frac{\partial}{\partial r}\left(r\frac{\partial C_4}{\partial r}\right) - \left(r^2 - \frac{d^2}{a^2} - 2\frac{r_e^2}{a^2}\ln\frac{ra}{d}\right)\frac{\partial C_4}{\partial z} = 0 \tag{B6}$$

$$\frac{1}{r}\frac{\partial}{\partial r}\left(r\frac{\partial C_3}{\partial r}\right) = 0 \tag{B7}$$

$$\frac{1}{r}\frac{\partial}{\partial r}\left(r\frac{\partial C_2}{\partial r}\right) = 0 \tag{B8}$$

$$\frac{1}{r}\frac{\partial}{\partial r}\left(r\frac{\partial C_1}{\partial r}\right) = \frac{\varphi C_1}{\theta + C_1} \tag{B9}$$

with boundary conditions

$$C_4(r, z) = 1 \quad z < 0 \tag{B10}$$

$$C_4\left(\frac{d}{a}, z\right) = C_w(z) \quad z > 0 \tag{B11}$$

$$\frac{\partial C_4}{\partial r}\Big|_{r=\frac{r_e}{a}} = 0 \tag{B12}$$

$$C_3\left(\frac{d}{a}, z\right) = C_w(z) \tag{B13}$$

$$\mathcal{D}_3\frac{\partial C_3}{\partial r}\Big|_{r=\frac{d}{a}} = \mathcal{D}_4\frac{\partial C_4}{\partial r}\Big|_{r=\frac{d}{a}} \tag{B14}$$

$$\gamma C_2\left(\frac{b}{a}, z\right) = C_3\left(\frac{b}{a}, z\right) \tag{B15}$$

$$\mathcal{D}_2\frac{\partial C_2}{\partial r}\Big|_{r=\frac{b}{a}} = \mathcal{D}_3\frac{\partial C_3}{\partial r}\Big|_{r=\frac{b}{a}} \tag{B16}$$

$$C_1(1, z) = \gamma C_2(1, z) \tag{B17}$$

$$\mathcal{D}_1\frac{\partial C_1}{\partial r}\Big|_{r=1} = \mathcal{D}_2\frac{\partial C_2}{\partial r}\Big|_{r=1} \tag{B18}$$

$$\frac{\partial C_1}{\partial r}\Big|_{r=0} = 0 \tag{B19}$$

The Péclet number for this configuration is defined as

$$\alpha_t = k\frac{Fa^3}{\pi(r_e^2 - d^2)\mathcal{D}_4} \tag{B20}$$

and φ and θ are defined as analogs of equations (29) and (30).

Equations (B6) to (B19) are solved by an iterative numerical finite difference scheme equivalent to that used for the enzyme-shell equations with Michaelis-Menten kinetics. Parameter values were the same as those employed in the enzyme-shell calculations with the addition of

$$\frac{r_e}{a} = 3.15 \quad \text{and} \quad \frac{\mathcal{D}_4}{\mathcal{D}_3} = 1.0$$

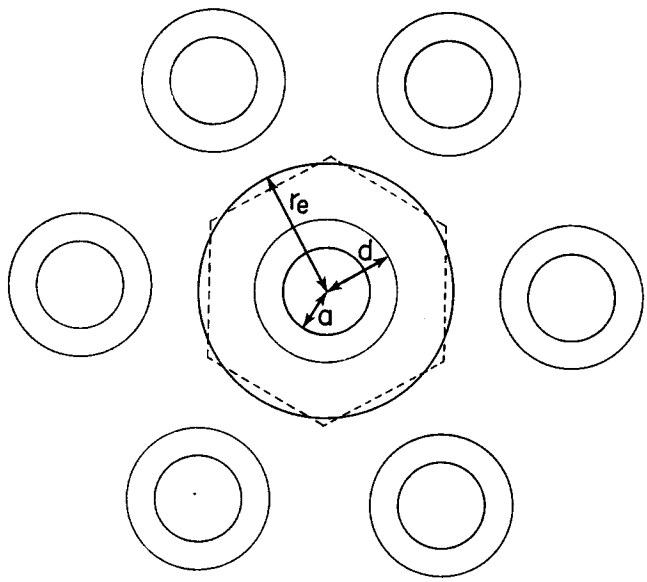

Fig. B1. Hollow fibers in equilateral triangular array.

Manuscript received June 21, 1973; revision received August 6 and accepted August 14, 1973.